

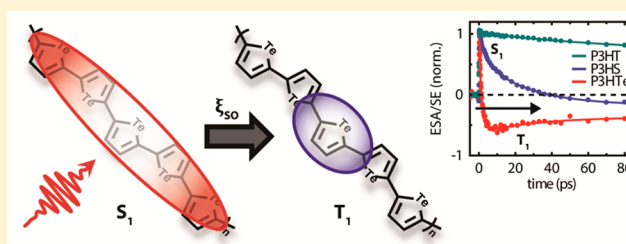
# Evidence for the Rapid Conversion of Primary Photoexcitations to Triplet States in Seleno- and Telluro- Analogues of Poly(3-hexylthiophene)

Ryan D. Pensack, Yin Song, Theresa M. McCormick,<sup>†</sup> Ashlee A. Jahnke, Jon Hollinger, Dwight S. Seferos,\* and Gregory D. Scholes\*

Department of Chemistry, University of Toronto, 80 St. George Street, Toronto, Ontario M5S 3H6, Canada

## S Supporting Information

**ABSTRACT:** Broadband pump–probe spectroscopy is used to examine the ultrafast photophysics of the  $\pi$ -conjugated polymers poly(3-hexylselenophene) (P3HS) and poly(3-hexyltellurophene) (P3HTE) in solution. An excited-state absorption feature that we attribute to a transition in the triplet manifold appears on the picosecond time scale. Density functional theory (DFT) and time-dependent density functional theory (TD-DFT) calculations support this assignment. The formation of triplets is consistent with significant fluorescence quenching observed in solutions of the neat polymers. Triplet formation occurs in  $\sim 26$  and  $\sim 1.8$  ps (upper limit) for P3HS and P3HTE, respectively. The successive decrease in fluorescence quantum efficiency and triplet formation time are consistent with intersystem crossing facilitated by the heavier selenium and tellurium atoms. These results strongly suggest that primary photoexcitations are rapidly converted into triplet states in P3HS and P3HTE.



## INTRODUCTION

Understanding the evolution of electronic excited states in conjugated polymers aids in their optimization for target applications, including organic solar cells.<sup>1,2</sup> Emerging materials, such as donor–acceptor copolymers with narrow optical gaps, currently represent the state-of-the-art in polymer: fullerene-based bulk-heterojunction solar cells with power conversion efficiencies approaching 10%.<sup>3,4</sup> The substitution of single atoms along the polymer chain represents an alternative strategy to tune the polymer optical properties. This approach is particularly advantageous, as it has the potential for minimal and/or more predictable changes to the polymer microstructural properties in the solid-state. This area of research was initially motivated by the development of poly(3-hexylselenophene) (P3HS) for organic optoelectronic applications.<sup>5,6</sup> Various polyselenophene<sup>7,8</sup> and polytellurophene<sup>9,10</sup> homopolymers, including poly(3-hexyltellurophene) (P3HTE),<sup>11</sup> were developed in the ensuing years. In addition to homopolymers, block, gradient, and statistical thiophene-selenophene copolymers have been reported<sup>12–14</sup> and selenium has been incorporated into donor–acceptor copolymers as a means to tune the electronic structure of these materials.<sup>15–21</sup> A ladder-type indacenodiselenophene-based polymer<sup>22</sup> and selenium-substituted PBDDTT-DPP polymer<sup>23</sup> represent particularly notable examples with corresponding polymer:fullerene bulk-heterojunction solar cells exhibiting power conversion efficiencies of  $\sim 7\%$ . A variety of heavy-atom substituted donor–acceptor polymers have been reported recently.<sup>24–26</sup> Details on the ultrafast photophysics of these materials and on

their charge photogeneration with an electron acceptor are only beginning to emerge. For example, studies on selenophene-based homopolymers indicate insufficient driving force for charge separation and fast nongeminate recombination in blends of these polymers with the fullerene PC<sub>61</sub>BM.<sup>27–30</sup>

A current bottleneck in organic photovoltaics is the mismatch between the singlet exciton diffusion length ( $\sim 5$ – $10$  nm) and corresponding optical absorption length ( $\sim 200$  nm). Several strategies exist to circumvent this issue with the most common being, by far, the bulk-heterojunction approach.<sup>31,32</sup> Utilizing triplet states based on their long lifetime and corresponding potential for long diffusion lengths has been suggested as a means to circumvent this issue.<sup>33</sup> Triplet exciton diffusion lengths can approach the micrometer-scale in single crystals and several tens of nanometers for more disordered solids.<sup>33–36</sup> The relatively small distance between chromophores and high degree of wave function overlap along the polymer chain suggests that triplet exciton diffusion may be relatively efficient in conjugated polymers.<sup>37–39</sup> The exchange energy, however, poses a significant energetic penalty that may prohibit the utilization of triplet states in solar energy conversion in molecular systems.<sup>34</sup> Singlet-fission sensitized solar cells represent an interesting means in which to circumvent losses introduced by the exchange energy, although careful design is still necessary to minimize any excess energy

Received: February 6, 2014

Revised: February 15, 2014

Published: February 17, 2014

required to overcome the exciton binding energy as the losses are doubled for the dissociation of two excitons.<sup>40</sup>

Here, we use broadband pump–probe spectroscopy to investigate the ultrafast photophysics of seleno- and telluro-analogues of P3HT, namely P3HS and P3HTE, as isolated chains in solution. We find an excited-state absorption feature appearing on the picosecond time scale in P3HS and P3HTE in a spectral region in close proximity to where the triplet excited-state absorption has been observed in other conjugated homopolymers, including P3HT. Density functional theory (DFT) and time-dependent density functional theory (TD-DFT) calculations suggest that this spectral feature is a transition in the triplet manifold. P3HS and P3HTE exhibit marked fluorescence quenching which indicates a significant nonradiative decay channel exists in these materials. Changes in the time constants associated with formation of this spectral feature for the material series P3HS, P3HT, and P3HTE are consistent with the order-of-magnitude changes in the rates anticipated for intersystem crossing facilitated by the heavy-atom effect. These results suggest that triplet states are rapidly formed in these materials following photoexcitation and subsequent intersystem crossing.

## EXPERIMENTAL SECTION

The polymers used for the present study were synthesized by Kumada catalyst transfer polymerization according to literature methods. P3HS and P3HTE have  $M_n$  values of 8.6 kDa (dispersity = 1.2) and 9.1 kDa (dispersity 1.8), respectively. The chemical structures of P3HS and P3HTE and the DFT optimized gas-phase structures of the representative octomer are displayed in Figure 1.

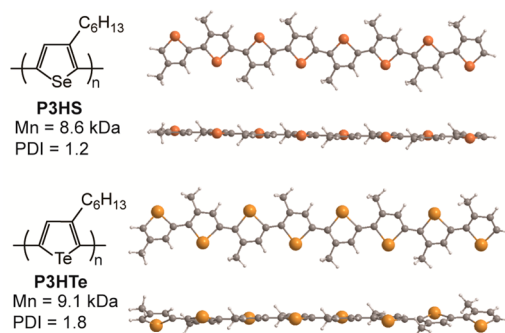


**Figure 1.** Chemical structures of poly(3-hexylselenophene) and poly(3-hexyltellurophene) along with optimized structure of the representative octomers (DFT, gas-phase).

Absorption spectra were measured on a Varian Cary 100 Bio Spectrophotometer (Varian Medical Systems, Inc., Palo Alto, CA). Scans were typically obtained in 2 nm intervals with 0.1 s averaging time with the slits set for 2 nm bandpass. Photoluminescence spectra were measured on a PTI Quantum Master Fluorimeter (Photon Technology International, Inc., Birmingham, NJ). Photoluminescence measurements were carried out with excitation and emission slits widths optimized to maximize sample signal. Solvents used for the different photoluminescence measurements are reported where appropriate. More details on the photoluminescence measurements can be found in the Supporting Information.

Broadband pump–probe experiments were carried out with a 5 kHz regeneratively amplified Ti:sapphire laser system

(Spectra-Physics, Santa Clara, CA) driving a custom-built noncollinear optical parametric amplifier (NOPA). The laser system consists of a Ti:sapphire oscillator seeding a Nd:YLF-pumped Ti:sapphire-based regenerative amplifier that delivers  $\sim 150$  fs pulses at  $\sim 800$  nm with an average power of  $\sim 3$  W. About one-third of the amplifier output is used to drive the NOPA. Details of the NOPA optical configuration have been reported previously.<sup>41</sup> The NOPA spectrum in each experiment was tuned to have sufficient spectral bandwidth to both excite the sample and probe spectral features at energies below the polymer optical gap. The NOPA pulses were compressed to less than  $\sim 50$  fs with a combination of a grating and prism compressor by monitoring the nonresonant solvent response of methanol placed at the sample position. A beamsplitter in the beam path separates the NOPA beam into pump and probe beams; the pump and probe pulse energies were controlled with a combination of a  $\lambda/2$  waveplate and thin-film polarizers. A detailed summation of the pump–probe setup is reported elsewhere.<sup>42</sup> Solutions for the pump–probe experiments were prepared with carbon disulfide as the solvent. The optical density of the lowest-energy absorption feature of these solutions was kept at or below  $\sim 0.3$ . The solution was contained in an evacuated 1 mm path length spectrophotometer cell that was deoxygenated via three freeze–pump–thaw cycles. Pump fluences were kept below  $\sim 150 \mu\text{J cm}^{-2}$  and are reported where appropriate.

## RESULTS

**Steady-State Spectroscopy.** Steady-state absorption and photoluminescence (PL) spectra of P3HS and P3HTE in carbon disulfide solution reveal a red-shift of the lowest allowed electronic transition with seleno- and telluro- substitution (Figure 2).<sup>6,11</sup> The absorption spectra of P3HS and P3HTE in

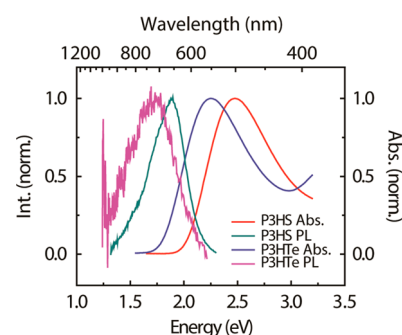


**Figure 2.** Steady-state absorption and PL spectra of P3HS (red and cyan) and P3HTE (blue and magenta) in carbon disulfide solution. Excitation energies for the PL measurements were 2.58 and 2.34 eV, respectively.

solution are structureless and lack any prominent low-energy features below the optical gap, indicating that the polymers are well dissolved and not aggregated. The PL spectrum of P3HS exhibits some vibronic structure. This is similar to what is observed in P3HT, although is hard to ascertain with confidence given the low signal levels (*vide infra*). The peak of the PL feature of P3HS in carbon disulfide is 1.89 eV and for P3HTE is roughly  $\sim 1.70$  eV. The difference between the absorption maximum and the maximum of the PL feature in P3HS and P3HTE is  $\sim 0.59$  eV ( $\sim 4,800 \text{ cm}^{-1}$ ) and  $\sim 0.57$  eV ( $\sim 4,600 \text{ cm}^{-1}$ ), respectively. These values are comparable to the apparent Stokes' shift of  $\sim 0.60$  eV ( $\sim 4,800 \text{ cm}^{-1}$ ) observed

for P3HT in chlorobenzene solution.<sup>43,44</sup> Deoxygenated solutions exhibited nearly the same photoluminescence intensity as solutions prepared in air without deoxygenation (Figure S1). Based on the similar apparent Stokes' shifts and lack of oxygen sensitivity, the photoluminescence feature is most likely fluorescence from singlet excitons.

The relative fluorescence intensity progressively decreases with seleno- and telluro- substitution. In order to gauge the extent of fluorescence quenching, the relative fluorescence quantum yield was determined. These measurements were performed on deoxygenated solutions with 1,2,4-trichlorobenzene as the solvent. For comparison, under our experimental conditions, the fluorescence quantum yield of P3HT is 0.30 and compares well with previously reported values.<sup>43</sup> The fluorescence quantum yields of P3HS and P3HTe are diminished significantly to  $\sim 4.2 \times 10^{-3}$  and  $\sim 1.4 \times 10^{-4}$ , respectively (Table S1).

**Broadband Pump–Probe Spectroscopy.** Figure 3 displays the broadband pump–probe spectra of P3HS. The

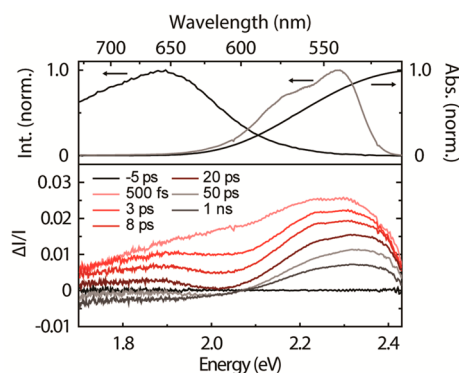


**Figure 3.** Broadband pump–probe spectra of P3HS excited with laser pulse centered at  $\sim 2.25$  eV and an incident excitation density of  $\sim 150 \mu\text{J}/\text{cm}^2$ . Laser pulse spectrum (gray line), steady-state PL and absorption spectra (black lines) are shown in the top panel above the transient spectra. Pump–probe time delays are indicated in the legend in the panel including the transient spectra.

transient spectra exhibit a prominent positive-going feature at  $>2.1$  eV. We attribute this feature to the ground-state bleach (GSB) as this overlaps with the steady-state absorption spectrum. We note that the shape of the GSB in the broadband pump–probe experiments is significantly distorted relative to the expected spectrum, most notably at the edges of the laser pulse spectrum. This is a result of the laser pulses employed in these experiments; the broadband pump–probe spectrum represents a convolution of the signal with the laser pulse spectrum. Another positive-going feature appears to red of the GSB feature. Based on its overlap with the steady-state PL spectrum, we attribute this feature to stimulated emission (SE). As the pump–probe time delay increases, we find that the SE feature shifts further to the red and evolves into a negative-going excited-state absorption (ESA) feature. Keeping in mind the unique positions of the spectral features appearing in the transient spectra of P3HS, these assignments and dynamics (i.e., evolution of SE to ESA) are consistent with those reported for isolated chains of P3HT.<sup>43,45</sup>

The broadband pump–probe spectra of P3HTe are displayed in Figure 4. We observe the same spectral features and overall dynamics in these data as in the broadband pump–probe spectra of P3HS. In contrast to both P3HS and P3HT,

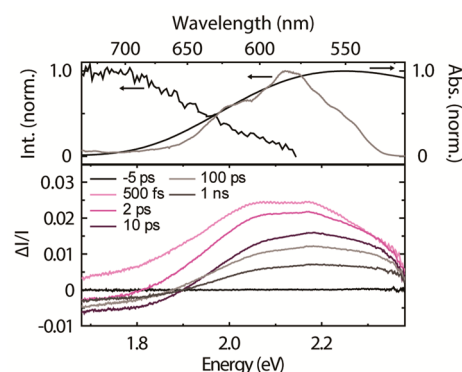


**Figure 4.** Broadband pump–probe spectra of P3HTe excited with laser pulse centered at  $\sim 2.12$  eV and an incident excitation density of  $\sim 100 \mu\text{J}/\text{cm}^2$ . Laser pulse (gray line), steady-state PL and absorption spectra (black lines) are shown in the top panel above the transient spectra. Pump–probe time delays are indicated in the legend in the panel including the transient spectra.

however, there is a notable lack of a prominent SE feature on any time scale for P3HTe. The spectral region where the SE should be found rapidly evolves to a negative-going ESA. Before proceeding to discuss these dynamics, we begin by discussing the assignment of the ESA spectral feature.

## DISCUSSION

**Assignment of Excited-State Absorption.** There are a few possible explanations for the nonradiative decay observed in these materials, including the formation of polaron pairs or triplet excitons. Thus, the excited-state absorption of P3HS and P3HTe could arise from either of these entities. A definitive assignment based on the transient spectra alone is not possible because the spectral profiles of positive and negative polaron and triplet excited-state absorptions appearing in this spectral window are very similar.<sup>46,47</sup> However, because polaron pair formation is inefficient in conjugated homopolymers in solution and the primary photoexcitations in heavy-atom containing polymers are anticipated to be excitonic in nature, the most plausible explanation for the entities giving rise to these spectral features are triplet excitons.

Polaron pair formation is ruled out as a possible pathway on the basis that the direct generation of carriers in homopolymers in solution is inefficient. Hendry et al., for example, found that the quantum yield for carrier generation in MEH-PPV is two orders-of-magnitude lower in a solution compared to films.<sup>48</sup> This is reflected in the transient conductivity observed in these measurements- the conductivity of MEH-PPV in solution decays to zero within 2 ps, while the conductivity in films persists on longer time scales.

The introduction of a heavy atom within the conjugated framework is not anticipated to substantially alter this picture. An abundance of evidence indicates that the primary photoexcitation in organometallic polymers is an exciton.<sup>49–51</sup> Two key experimental observations lend substantial support to this claim: (i) a large energy difference between fluorescence and phosphorescence in platinum and palladium polyynes, or acetylides, indicating a large exchange energy ( $>0.8$  eV) and Coulomb interaction as would be anticipated for an excitonic photoexcitation;<sup>49,50</sup> and (ii) the photoconductive and photovoltaic responses are similar to other excitonic materials, such as PPV.<sup>51</sup> Because the exciton binding energy in these materials



is typically several tenths of an electronvolt,<sup>52–56</sup> a significant population of positive and negative polarons is not anticipated at ambient temperature ( $\sim 0.025$  eV) without a suitable driving force.

On the basis of the marked fluorescence quenching with seleno- and telluro- substitution, the appearance of an ESA feature on the picosecond time scale, and based on the discussion above that polaron formation is unlikely in solution, we assign the ESA to a triplet  $T_1 \rightarrow T_n$  transition. We have carried out density functional theory (DFT) geometry optimizations and time-dependent density-functional theory (TD-DFT) calculations on eight repeat units of 3-methyl selenophene and tellurophene (see Supporting Information for details) to provide further guidance for this assignment (Figure 5). The calculated  $S_0 \rightarrow S_1$  transition energies agree with the

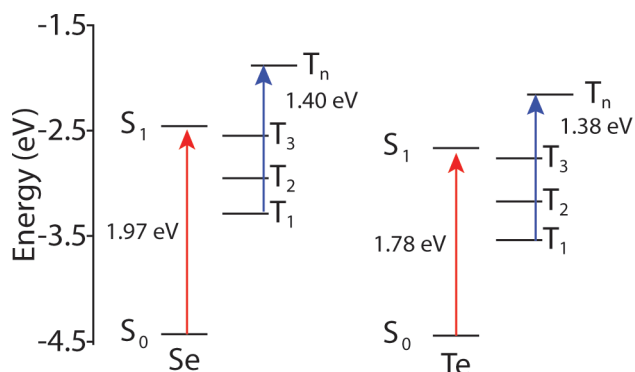


**Figure 5.** TD-DFT excitations for ground,  $S_0$ , to first excited single state,  $S_1$  (red arrow). The  $S_0$  state is aligned in the diagram with the calculated HOMO energy level.  $T_1$ ,  $T_2$ , and  $T_3$  energies are the relative triplet excitation energies. The  $T_1$  to  $T_n$  excitation (blue arrow) is represented by the transition with highest oscillator strength obtained from the TD-DFT calculation on the optimized geometry of the triplet. Eight repeat units of 3-methyl selenophene and tellurophene were used for the calculations. Absolute energies are referenced to the HOMO level.

experimentally observed trend of decreasing optical gap transition energies with substitution of selenium and tellurium. On the other hand, the calculated  $T_1 \rightarrow T_n$  transition energies do not change substantially with selenium and tellurium substitution and are quite similar to the experimentally determined  $T_1 \rightarrow T_n$  transition in P3HT ( $\sim 1.45$  eV).<sup>43,57</sup>

The assignment of a triplet excited-state absorption in this spectral region is further supported by previous work indicating the  $T_1 \rightarrow T_n$  transition is relatively invariant to chemical structure in conjugated homopolymers.<sup>34</sup> A wide range of conjugated homopolymers exhibit a  $T_1 \rightarrow T_n$  transition in the proximity of  $\sim 1.5$  eV including polyfluorenes, polyphenylenevinyls, ladder-type polyphenylenes and platinum acetylides.<sup>34</sup> As discussed by Köhler and Bässler, the physical origin for the relative invariance of the  $T_1 \rightarrow T_n$  transition energy is related, in part, to a relatively consistent singlet–triplet splitting measured for various conjugated homopolymers.<sup>34</sup> For example, using a combined pulse radiolysis and triplet energy transfer technique, Monkman et al. determined a singlet–triplet splitting value of  $\sim 0.7$  eV for a series of conjugated homopolymers including polythiophenes, polyphenylenevinyls, and polyfluorenes.<sup>58</sup> Köhler et al. directly measured the singlet–triplet splitting via luminescence measurements and consistently obtained a value of  $\sim 0.7$  eV for several different

phenyleneethynylene polymers including their platinum-containing analogs.<sup>59</sup> These results indicate that the exchange energy is relatively invariant to chemical structure in these various classes of conjugated homopolymers.<sup>34</sup> This is thought to arise from similar singlet and triplet wave function overlap along the polymer chain that does not vary with chemical composition.<sup>34</sup> We note that these observations are not universal for all organic conjugated systems.<sup>34,60</sup> The singlet–triplet splitting can vary substantially in molecules and oligomers in which the dimensionality can be readily varied,<sup>60</sup> and in materials in which the overlap of electron and hole wave functions is altered such as in carbazole-containing materials that contain nonbonding orbitals<sup>61</sup> and donor–acceptor oligomers and copolymers<sup>62</sup> (see refs 34 and 60 for a more detailed discussion). Given the minimal chemical modification of the polymers in the present study, these materials should fit within the picture elucidated for polythiophenes and conjugated homopolymers more generally.<sup>34,58,59</sup>

Having assigned the excited-state absorption feature appearing at the red edge of our spectral window to a transition in the triplet manifold, we proceed with a comparative analysis of the dynamics associated with P3HT, P3HS, and P3HTe in this spectral region (broadband pump–pump spectra of P3HT are included in the Supporting Information).

**Temporal Evolution of Stimulated Emission/Excited-State Absorption.** The kinetics traces in the spectral region of the SE/ESA for P3HT, P3HS, and P3HTe at probe energies of 2.08, 1.89, and 1.75 eV, respectively, are considered next (Figure 6). These particular probe energies minimize the effects of time-dependent spectral shifts and amplitude changes in this spectral region because they are as close to the steady-state PL peak maximum as possible (Figure S3). We were unable to analyze the P3HTe data set at the PL maximum as these data were at the limits of our spectral window, and so we analyzed this particular data set slightly blue-shifted ( $\sim 0.05$  eV) relative to the steady-state fluorescence maximum. We found that carrying out the analysis for P3HTe as far blue-shifted as  $\sim 0.1$  eV did not significantly alter the results, other than changing the relative amplitude of the different decay components. Upon inspection of Figure 6, it is apparent that the time scale of formation of the ESA spectral feature changes by a few orders-of-magnitude upon the introduction of selenium and tellurium into the polymer backbone.

We begin by discussing the dynamics associated with this spectral region in P3HT because the dynamics of P3HT have been well characterized.<sup>43–45,63–65</sup> The decay of the SE spectral feature of P3HT is wavelength dependent and highly nonexponential.<sup>44,63–65</sup> The dynamic Stokes' shift and decay of the SE feature of P3HT has multiple time constants encompassing several orders-of-magnitude ranging from subpicosecond to several hundreds of picoseconds. In conjugated polymers, the dynamic Stokes' shift is attributed to a combination of a subpicosecond component that is associated with relaxation through a manifold of delocalized exciton states and self-localization due to electron–nuclear coupling<sup>66–71</sup> along with longer time scale intrachain electronic energy transfer and excited-state conformational relaxation.<sup>34,45,63,70–78</sup> We fit the decay of the SE spectral feature at a probe energy of 2.08 eV with a sum of four exponentials allowing the longest time constant to vary, while constraining the shortest time constants to those reported by Banerji et al.<sup>44</sup> This approach was necessary to compensate for artifacts in the

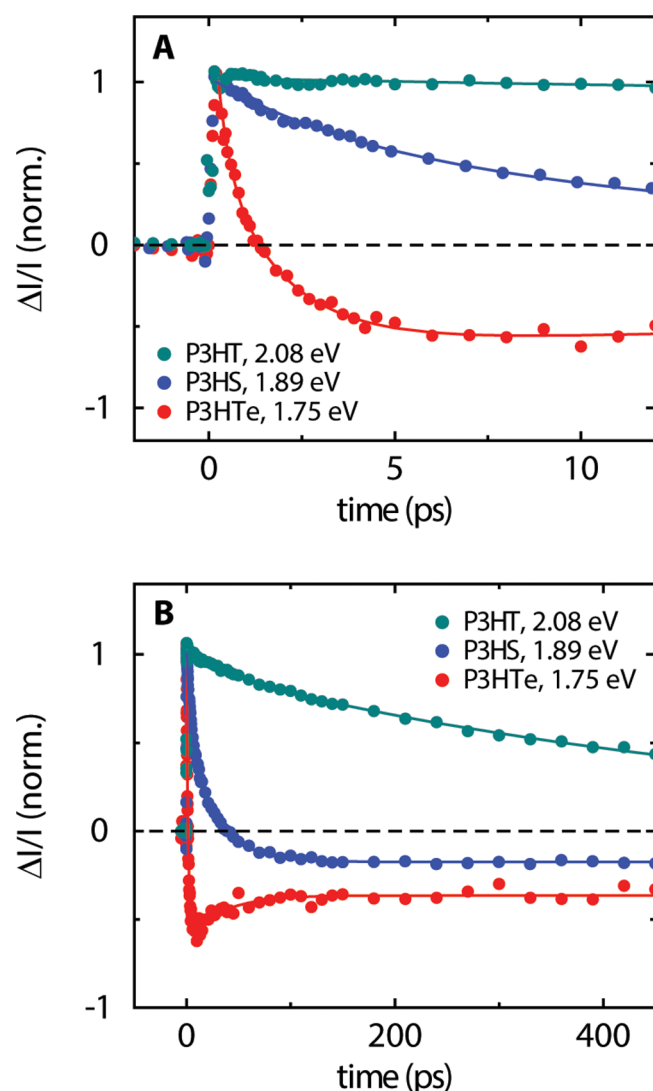


**Figure 6.** Temporal evolution of SE/ESA spectral region for P3HT, P3HS, and P3HTe as assayed at probe energies of 2.08, 1.89, and 1.75 eV, respectively, on (A) picosecond and (B) hundreds of picoseconds time scales. The data represent the mean at these probe energies over a range of  $\pm 0.025$  eV and have been normalized to the maximum signal amplitude near the time origin. Incident excitation density was  $\sim 50 \mu\text{J}/\text{cm}^2$  for each experiment. Solid lines are multiexponential fits discussed in the text.

broadband pump–probe experiment that bias the subtle picosecond and subpicosecond time scale spectral shifts. These artifacts are a result of the degenerate nature of the pump and probe pulses and include various physical phenomena such as the coherent spike, impulsive stimulated Raman scattering of the solvent, and the optical Kerr effect. The longest time constant for P3HT that we obtain from the fitting procedure is  $\sim 600$  ps, which is consistent with the photoluminescence lifetime of  $\sim 500$  ps measured previously for singlet excitons in isolated chains of P3HT.<sup>43,44,56,65,79</sup>

The evolution in the spectral region of the SE/ESA spectral features in P3HS and P3HTe is also nonexponential. We fit the evolution of SE into ESA in this spectral region with a biexponential function allowing the amplitudes and time constants to vary and allowing for a nonzero offset. The P3HS dynamics are well described by a biexponential function with time constants of 3.9 and 26 ps contributing 37% and 63%

to the decay, respectively. A single exponential fit to the P3HS dynamics resulted in a visibly poor fit and an order-of-magnitude larger  $\chi^2$  (Figure S4). The decay of P3HTe is also well-described by a biexponential function with time constants of 0.3 and 1.8 ps contributing 49% and 51% to the decay, respectively. As the focus of the present discussion is to highlight and discuss trends in the time scale that the ESA spectral feature appears, we take the latter value from this analysis as an upper limit to the formation time. We thus find an order-of-magnitude difference in the time constants associated with the formation of the ESA spectral feature in P3HS and P3HTe. The weighted sum of the time constants obtained from the fits are 18 and 1.1 ps for P3HS and P3HTe, respectively; these time constants exhibit an order-of-magnitude difference, as well. Thus, there is an order-of-magnitude difference between the selenium and tellurium polymer regardless of choice of time constants. We will discuss the longer time scale evolution in P3HTe further below, briefly mentioning that these data were fit with an exponential function with a time constant of several tens of picoseconds.

Based on our assignment of this spectral feature to the triplet  $T_1 \rightarrow T_n$  absorption and the order-of-magnitude changes in the time scale associated with its formation in the selenium and tellurium polymers, we interpret these observations as an increased rate of intersystem crossing. Kraabel et al. spectrally resolved both  $S_1 \rightarrow S_n$  and  $T_1 \rightarrow T_n$  ESA features in the transient spectra of P3HT and poly(3-octylthiophene).<sup>56</sup> These authors determined that intersystem crossing occurs at a rate of  $1.2 \text{ ns}^{-1}$  using a kinetic model that takes into account the evolution of singlet and triplet populations. Beljonne et al. carried out quantum-chemical calculations to provide further insight into the mechanism of intersystem crossing in oligo- and polythiophenes.<sup>80,81</sup> Their calculations indicated that two nearby, quasi-degenerate triplet states (relative to  $S_1$ ) are the only states in the triplet manifold likely to play a role in the intersystem crossing in oligothiophenes.<sup>81</sup> These authors proposed two requirements for intersystem crossing in conjugated polymers (on the basis of radiationless transition theory) that are, in addition to dynamic conformational disorder, necessary to circumvent the symmetry constraints forbidding intersystem crossing:<sup>81</sup> (i) a sizable spin–orbit coupling with  $S_1$  and (ii) a triplet state in the triplet manifold quasi-degenerate with the  $S_1$  state.

The magnitude of the changes in the rate of formation of the ESA spectral feature that we observe in P3HS and P3HTe are consistent with the order-of-magnitude changes anticipated in the rate of intersystem crossing facilitated by increasingly heavier atoms. The “heavy-atom” effect is related to a modification of the matrix element for spin–orbit coupling via the introduction of a nucleus into the molecular framework with a large effective nuclear charge. This modification of the matrix element enables significant mixing of singlet and triplet wave function character. The strength of spin–orbit coupling is proportional to the atomic number to the fourth power, although this correlation is only exact for atomic systems as spin–orbit coupling is a local effect.<sup>82</sup> For the S, Se, and Te atoms incorporated into the polymers in the present study, the spin–orbit coupling is expected to increase substantially. With these atoms in close proximity to the  $\pi$ -conjugated network, the first criterion of a perturbation enabling significant mixing of singlet and triplet wave function character is met. In addition, quasi-degenerate singlet and triplet states are required for facile intersystem crossing. The TD-DFT calculations indicate that

there are nearby, quasi-degenerate triplet states close in energy to the  $S_1$  state in P3HS and P3HTE that would readily facilitate intersystem crossing in each polymer.

Assuming the intrinsic radiative lifetime in these materials is similar to the  $\sim 2$  ns lifetime reported for P3HT<sup>56</sup> and that internal conversion from  $S_1$  to  $S_0$  is not the major rate determining deactivation pathway, we estimate the lifetime of singlet excitons in P3HT, P3HS, and P3HTE to be  $\sim 600$ ,  $\sim 8$ , and  $\sim 0.3$  ps, respectively, based on the fluorescence quantum yields reported in Table S1. These values are consistent with the general variation in the time scale that the ESA feature forms in each polymer in the pump–probe experiment. Although the estimated singlet lifetime does not quantitatively match the time constants obtained from the pump–probe experiments, the approximate relative differences are quite consistent. The lack of quantitative agreement may be a result of a variety of factors including limitations in the assumptions behind the singlet exciton lifetime estimation, factors complicating the interpretation of the time constants obtained directly from the pump–probe data, and/or the different solvents employed in the pump–probe and steady-state measurements. Taking the latter point, for example, we note that the lowest-energy absorption maximum of P3HS in  $CS_2$  is 2.48 eV, while in 1,2,4-trichlorobenzene the absorption is red-shifted with the maximum appearing at 2.44 eV. Solvatochromic effects could conceivably alter the electronic manifold of the polymer in a manner varying the proximity of quasi-degenerate triplet and singlet energy levels, which would alter the rate of intersystem crossing. Regardless, this simple correlation between the steady-state observables and the time constants obtained from the pump–probe experiment is consistent with a single unimolecular or first-order process, such as intersystem crossing, becoming the dominant process that determines the photophysical pathway of primary photoexcitations in these materials. Fluence dependent measurements are consistent with this being a unimolecular process (Figure S5, S6). Transient absorption measurements on other heavy-atom containing oligomers and polymers, such as the platinum acetylides, indicate similarly rapid picosecond time scale intersystem crossing.<sup>39,83–88</sup>

It is worth highlighting and discussing the decay of the ESA feature in P3HTE on the several tens of picoseconds time scale. There are several possible explanations for the decay. One is the annihilation of a large population of triplet states generated via either intersystem crossing or singlet fission. P3HTE has potential as a singlet fission material given the relatively low optical absorption energy ( $\sim 1.7$  eV) and anticipated large singlet–triplet splitting ( $\sim 0.7$  eV). Fluence dependence measurements indicate that the rate of decay does not increase with increasing fluence (Figure S6). These results indicate that the decay is not a result of a bimolecular mechanism, at least over the fluence range measured. Ruling out a geminate recombination mechanism is more challenging based on these results alone. A close inspection of the pump–probe spectra displayed in Figure 4 indicates that a change in an isosbestic point between the ESA and the GSB occurs on a similar time scale as the decay of the amplitude of the ESA spectral feature. Although admittedly speculative, a change in the isosbestic point in this manner may more likely be a result of a spectral shift or change in oscillator strength rather than a change in population, indicating that both of the explanations presented above are unlikely. For example, the changes in the P3HTE transient spectra on the tens of picoseconds time scale could be

a result of a time-dependent shift of the  $T_1 \rightarrow T_n$  transition arising from either conformational relaxation or triplet electronic energy transfer. This interpretation is consistent with the  $\sim 15$  ps time scale reported for conformational relaxation of singlet excitons in poly[3-(2,5-diocylphenyl)-thiophene]<sup>75</sup> or the  $\sim 30$  ps time scale reported for intrachain triplet exciton diffusion in platinum acetylide oligomers.<sup>39</sup>

## CONCLUSIONS

In conclusion, we reported on the first study of the ultrafast photophysics of two recently introduced seleno- and telluro-analogues of poly(3-hexylthiophene), namely, poly(3-hexylselenophene) and poly(3-hexyltellurophene). Rapid formation of an excited-state absorption in the triplet manifold is observed in these polymers. The order-of-magnitude changes in the time scale associated with formation of this spectral feature with seleno- and telluro- substitution is consistent with the order-of-magnitude changes in the rate of intersystem crossing anticipated with substitution of successively heavier atoms. The present findings provide useful guidance for the time scales of triplet generation in P3HS and P3HTE and provide motivation for a more comprehensive evaluation of the photophysics in these materials. These materials may represent attractive candidates to exploit charge photogeneration via triplet excitons, as in the platinum acetylides, with the advantage of leveraging the extensive materials know-how of P3HT including the molecular packing arrangement and ability to predictably mix with a fullerene-based electron acceptor.

## ASSOCIATED CONTENT

### Supporting Information

Additional experimental details, information on computational methods, results of fluorescence quantum yield measurements, and broadband pump–probe data are included in the Supporting Information. This material is available free of charge via the Internet at <http://pubs.acs.org>.

## AUTHOR INFORMATION

### Corresponding Authors

\*E-mail: [greg.scholes@utoronto.ca](mailto:greg.scholes@utoronto.ca).

\*E-mail: [dseferos@chem.utoronto.ca](mailto:dseferos@chem.utoronto.ca).

### Present Address

<sup>†</sup>Department of Chemistry, Portland State University, P.O. Box 751, Portland, OR 97207, USA.

### Notes

The authors declare no competing financial interest.

## ACKNOWLEDGMENTS

G.D.S. acknowledges financial support for this work from the U.S. AFOSR (FA9550-13-1-0005) and the NSERC of Canada. D.S.S. is grateful to NSERC, the CFI, The Ontario Research Fund, DuPont (for a Young Professor Grant), and the Alfred P. Sloan Foundation (for a Research Fellowship in Chemistry). A.A.J. is grateful for the financial support of the Colin Hahnemann Bayley Fellowship. R.D.P. would like to thank Daniel Turner, Paul Arpin, and Scott McClure for the design and original implementation of the pump–probe spectrometer, Yoichi Kobayashi for design and use of the evacuated spectrophotometer cell, Tak Kee for stimulating discussion, and the referees for valuable comments.



## REFERENCES

- (1) Brédas, J.-L.; Norton, J. E.; Cornil, J.; Coropceanu, V. Molecular Understanding of Organic Solar Cells: The Challenges. *Acc. Chem. Res.* **2009**, *42*, 1691–1699.
- (2) Clarke, T. M.; Durrant, J. R. Charge Photogeneration in Organic Solar Cells. *Chem. Rev.* **2010**, *110*, 6736–6767.
- (3) He, Z.; Zhong, C.; Su, S.; Xu, M.; Wu, H.; Cao, Y. Enhanced Power-Conversion Efficiency in Polymer Solar Cells Using an Inverted Device Structure. *Nat. Photon.* **2012**, *6*, 593–597.
- (4) You, J.; Dou, L.; Yoshimura, K.; Kato, T.; Ohya, K.; Moriarty, T.; Emery, K.; Chen, C.-C.; Gao, J.; Li, G.; et al. A Polymer Tandem Solar Cell with 10.6% Power Conversion Efficiency. *Nat. Commun.* **2013**, *4*, 1446.
- (5) Ballantyne, A. M.; Chen, L.; Nelson, J.; Bradley, D. D. C.; Astuti, Y.; Maurano, A.; Shuttle, C. G.; Durrant, J. R.; Heeney, M.; Duffy, W.; et al. Studies of Highly Regioregular Poly(3-hexylselenophene) for Photovoltaic Applications. *Adv. Mater.* **2007**, *19*, 4544–4547.
- (6) Heeney, M.; Zhang, W.; Crouch, D. J.; Chabinyc, M. L.; Gordeyev, S.; Hamilton, R.; Higgins, S. J.; McCulloch, I.; Skabara, P. J.; Sparrowe, D.; et al. Regioregular Poly(3-hexylselenophene): A Low Band Gap Organic Hole Transporting Polymer. *Chem. Commun.* **2007**, *47*, 5061–5063.
- (7) Patra, A.; Bendikov, M. Polyselenophenes. *J. Mater. Chem.* **2010**, *3*, 422–433.
- (8) Patra, A.; Wijsboom, Y. H.; Leitun, G.; Bendikov, M. Tuning the Band Gap of Low-Band-Gap Polyselenophenes and Polythiophenes: The Effect of the Heteroatom. *Chem. Mater.* **2011**, *23*, 896–906.
- (9) Jahnke, A. A.; Howe, G. W.; Seferos, D. S. Polytellurophenes with Properties Controlled by Tellurium-Coordination. *Angew. Chem., Int. Ed.* **2010**, *49*, 10140–10144.
- (10) Jahnke, A. A.; Seferos, D. S. Polytellurophenes. *Macromol. Rapid Commun.* **2011**, *32*, 943–951.
- (11) Jahnke, A. A.; Djukic, B.; McCormick, T. M.; Domingo, E. B.; Hellmann, C.; Lee, Y.; Seferos, D. S. Poly(3-alkyltellurophene)s Are Solution-Processable Polyheterocycles. *J. Am. Chem. Soc.* **2013**, *135*, 951–954.
- (12) Hollinger, J.; Jahnke, A. A.; Coombs, N.; Seferos, D. S. Controlling Phase Separation and Optical Properties in Conjugated Polymers through Selenophene–Thiophene Copolymerization. *J. Am. Chem. Soc.* **2010**, *132*, 8546–8547.
- (13) Palermo, E. F.; McNeil, A. J. Impact of Copolymer Sequence on Solid-State Properties for Random, Gradient and Block Copolymers containing Thiophene and Selenophene. *Macromolecules* **2012**, *45*, 5948–5955.
- (14) Hollinger, J.; Sun, J.; Gao, D.; Karl, D.; Seferos, D. S. Statistical Conjugated Polymers Comprising Optoelectronically Distinct Units. *Macromol. Rapid Commun.* **2013**, *34*, 437–441.
- (15) Saadeh, H. A.; Lu, L.; Bullock, J. E.; Wang, W.; Carsten, B.; Yu, L. Polyselenopheno[3,4-*b*]selenophene for Highly Efficient Bulk Heterojunction Solar Cells. *ACS Macro Lett.* **2012**, *1*, 361–365.
- (16) Beaupré, S.; Pron, A.; Drouin, S. H.; Najari, A.; Mercier, L. G.; Robitaille, A.; Leclerc, M. Thieno-, Furo-, and Selenopheno[3,4-*c*]pyrrole-4,6-dione Copolymers: Effect of the Heteroatom on the Electrooptical Properties. *Macromolecules* **2012**, *45*, 6906–6914.
- (17) Kim, B.; Yeom, H. R.; Yun, M. H.; Kim, J. Y.; Yang, C. A Selenophene Analogue of PCDTBT: Selective Fine-Tuning of LUMO to Lower of the Bandgap for Efficient Polymer Solar Cells. *Macromolecules* **2012**, *45*, 8658–8664.
- (18) Alghamdi, A. A. B.; Watters, D. C.; Yi, H.; Al-Faifi, S.; Almeataq, M. S.; Coles, D.; Kingsley, J.; Lidzey, D. G.; Iraqi, A. Selenophene vs. Thiophene in Benzothiadiazole-based Low Energy Gap Donor-Acceptor Polymers for Photovoltaic Applications. *J. Mater. Chem. A* **2013**, *1*, 5165–5171.
- (19) Zhuang, W.; Zhen, H.; Kroon, R.; Tang, Z.; Hellström, S.; Hou, L.; Wang, E.; Gedefaw, D.; Inganäs, O.; Zhang, F.; et al. Molecular Orbital Energy Level Modulation Through Incorporation of Selenium and Fluorine Into Conjugated Polymers for Organic Photovoltaic Cells. *J. Mater. Chem. A* **2013**, *1*, 13422–13425.
- (20) Chang, H.-H.; Tsai, C.-E.; Lai, Y.-Y.; Liang, W.-W.; Hsu, S.-L.; Hsu, C.-S.; Cheng, Y.-J. A New Pentacyclic Indacenodiselenophene Arene and Its Donor–Acceptor Copolymers for Solution-Processable Polymer Solar Cells and Transistors: Synthesis, Characterization, and Investigation of Alkyl/Alkoxy Side-Chain Effect. *Macromolecules* **2013**, *46*, 7715–7726.
- (21) Wang, D. H.; Pron, A.; Leclerc, M.; Heeger, A. J. Additive-Free Bulk-Heterojunction Solar Cells with Enhanced Power Conversion Efficiency, Comprising a Newly Designed Selenophene–Thienopyrroliodone Copolymer. *Adv. Funct. Mater.* **2013**, *23*, 1297–1304.
- (22) Intemann, J. J.; Yao, K.; Yip, H.-L.; Xu, Y.-X.; Li, Y.-X.; Liang, P.-W.; Ding, F.-Z.; Li, X.; Jen, A.K.-Y. Molecular Weight Effect on the Absorption, Charge Carrier Mobility, and Photovoltaic Performance of an Indacenodiselenophene-Based Ladder-Type Polymer. *Chem. Mater.* **2013**, *25*, 3188–3195.
- (23) Dou, L.; Chang, W.-H.; Gao, J.; Chen, C.-C.; You, J.; Yang, Y. A Selenium-Substituted Low-Bandgap Polymer with Versatile Photovoltaic Applications. *Adv. Mater.* **2013**, *25*, 825–831.
- (24) Gibson, G. L.; McCormick, T. M.; Seferos, D. S. Atomistic Band Gap Engineering in Donor–Acceptor Polymers. *J. Am. Chem. Soc.* **2012**, *134*, 539–547.
- (25) He, G.; Kang, L.; Delgado, W. T.; Shynkaruk, O.; Ferguson, M. J.; McDonald, R.; Rivard, E. The Marriage of Metallocycle Transfer Chemistry with Suzuki–Miyaura Cross-Coupling To Give Main Group Element-Containing Conjugated Polymers. *J. Am. Chem. Soc.* **2013**, *135*, 5360–5363.
- (26) Gibson, G. L.; McCormick, T. M.; Seferos, D. S. Effect of Group-14 and Group-16 Substitution on the Photophysics of Structurally Related Donor–Acceptor Polymers. *J. Phys. Chem. C* **2013**, *117*, 16606–16615.
- (27) Ohkita, H.; Cook, S.; Astuti, Y.; Duffy, W.; Tierney, S.; Zhang, W.; Heeney, M.; McCulloch, I.; Nelson, J.; Bradley, D. D. C.; et al. Charge Carrier Formation in Polythiophene/Fullerene Blend Films Studied by Transient Absorption Spectroscopy. *J. Am. Chem. Soc.* **2008**, *130*, 3030–3042.
- (28) Ballantyne, A. M.; Ferenczi, T. A. M.; Campoy-Quiles, M.; Clarke, T. M.; Maurano, A.; Wong, K. H.; Zhang, W.; Stingelin-Stutzmann, N.; Kim, J.-S.; Bradley, D. D. C.; et al. Understanding the Influence of Morphology on Poly(3-hexylselenothiophene):PCBM Solar Cells. *Macromolecules* **2010**, *43*, 1169–1174.
- (29) Clarke, T. M.; Ballantyne, A. M.; Tierney, S.; Heeney, M.; Duffy, W.; McCulloch, I.; Nelson, J.; Durrant, J. R. Charge Photogeneration in Low Band Gap Polyselenophene/Fullerene Blend Films. *J. Phys. Chem. C* **2010**, *114*, 8068–8075.
- (30) Maurano, A.; Shuttle, C. G.; Hamilton, R.; Ballantyne, A. M.; Nelson, J.; Zhang, W.; Heeney, M.; Durrant, J. R. Transient Optoelectronic Analysis of Charge Carrier Losses in a Selenophene/Fullerene Blend Solar Cell. *J. Phys. Chem. C* **2011**, *115*, 5947–5957.
- (31) Halls, J. J. M.; Walsh, C. A.; Greenham, N. C.; Marseglia, E. A.; Friend, R. H.; Moratti, S. C.; Holmes, A. B. Efficient Photodiodes from Interpenetrating Polymer Networks. *Nature* **1995**, *376*, 498–500.
- (32) Yu, G.; Gao, J.; Hummelen, J. C.; Wudl, F.; Heeger, A. J. Polymer Photovoltaic Cells: Enhanced Efficiencies via a Network of Internal Donor–Acceptor Heterojunctions. *Science* **1995**, *270*, 1789–1791.
- (33) Yost, S. R.; Hontz, E.; Yeganeh, S.; Van Voorhis, T. Triplet vs Singlet Energy Transfer in Organic Semiconductors: The Tortoise and the Hare. *J. Phys. Chem. C* **2012**, *116*, 17369–17377.
- (34) Köhler, A.; Bässler, H. Triplet States in Organic Semiconductors. *Mater. Sci. Eng. R* **2009**, *66*, 71–109.
- (35) Najafav, H.; Lee, B.; Zhou, Q.; Feldman, L. C.; Podzorov, V. Observation of Long-Range Exciton Diffusion in Highly Ordered Organic Semiconductors. *Nat. Mater.* **2010**, *9*, 938–943.
- (36) Mikhnenko, O. V.; Ruiter, R.; Blom, P. W. M.; Loi, M. A. Direct Measurement of the Triplet Exciton Diffusion Length in Organic Semiconductors. *Phys. Rev. Lett.* **2012**, *108*, 137401.
- (37) Devi, L. S.; Al-Suti, M. K.; Dosche, C.; Khan, M. S.; Friend, R. H.; Köhler, A. Triplet Energy Transfer in Conjugated Polymers. I.

Experimental Investigation of a Weakly Disordered Compound. *Phys. Rev. B* **2008**, *78*, 045210.

(38) Köhler, A.; Bässler, H. What Controls Triplet Exciton Transfer in Organic Semiconductors? *J. Mater. Chem.* **2011**, *21*, 4003–4011.

(39) Keller, J. M.; Glusac, K. D.; Danilov, E. O.; McIlroy, S.; Sreearuthai, P.; Cook, A. R.; Jiang, H.; Miller, J. R.; Schanze, K. S. Negative Polaron and Triplet Exciton Diffusion in Organometallic “Molecular Wires”. *J. Am. Chem. Soc.* **2011**, *133*, 11289–11298.

(40) Ehrler, B.; Wilson, M. W. B.; Rao, A.; Friend, R. H.; Greenham, N. C. Singlet Exciton Fission-Sensitized Infrared Quantum Dot Solar Cells. *Nano Lett.* **2012**, *12*, 1053–1057.

(41) Turner, D. B.; Wilk, K. E.; Curmi, P. M. G.; Scholes, G. D. Comparison of Electronic and Vibrational Coherence Measured by Two-Dimensional Electronic Spectroscopy. *J. Phys. Chem. Lett.* **2011**, *2*, 1904–1911.

(42) McClure, S. D.; Turner, D. B.; Arpin, P. C.; Mirkovic, T.; Scholes, G. D. Coherent Oscillations in the PC577 Cryptophyte Antenna Occur in the Excited Electronic State. *J. Phys. Chem. B* **2014**, *118*, 1296–1308.

(43) Cook, S.; Furube, A.; Katoh, R. Analysis of the Excited States of Regioregular Polythiophene P3HT. *Energy Env. Sci* **2008**, *1*, 294–299.

(44) Banerji, N.; Cowan, S.; Vauthey, E.; Heeger, A. J. Ultrafast Relaxation of the Poly(3-hexylthiophene) Emission Spectrum. *J. Phys. Chem. C* **2011**, *115*, 9726–9739.

(45) Busby, E.; Carroll, E. C.; Chinn, E. M.; Chang, L.; Moulé, A. J.; Larsen, D. S. Excited-State Self-Trapping and Ground-State Relaxation Dynamics in Poly(3-hexylthiophene) Resolved with Broadband Pump–Dump–Probe Spectroscopy. *J. Phys. Chem. Lett.* **2011**, *2*, 2764–2769.

(46) Burrows, H. D.; Miguel, M. D.; Monkman, A. P.; Hamblett, I.; Navaratnam, S. Transient Absorption Spectra of Triplet States and Charge Carriers of Conjugated Polymers. *J. Mol. Struct.* **2001**, *563*, 41–50.

(47) Takeda, N.; Miller, J. R. Poly(3-decylthiophene) Radical Anions and Cations in Solution: Single and Multiple Polarons and Their Delocalization Lengths in Conjugated Polymers. *J. Phys. Chem. B* **2012**, *116*, 14715–14723.

(48) Hendry, E.; Koeberg, M.; Schins, J. M.; Nienhuys, H. K.; Sundström, V.; Siebbeles, L. D. A.; Bonn, M. Interchain Effects in the Ultrafast Photophysics of a Semiconducting Polymer: THz Time-Domain Spectroscopy of Thin Films and Isolated Chains in Solution. *Phys. Rev. B* **2005**, *71*, 125201.

(49) Wittmann, H. F.; Fuhrmann, K.; Friend, R. H.; Khan, M. S.; Lewis, J. Optical Excitations in Transition Metal Containing Poly-ynes. *Synth. Met.* **1993**, *55*, 56–61.

(50) Wittmann, H. F.; Friend, R. H.; Khan, M. S.; Lewis, J. Optical Spectroscopy of Platinum and Palladium Containing Poly-ynes. *J. Chem. Phys.* **1994**, *101*, 2693–2698.

(51) Köhler, A.; Wittmann, H. F.; Friend, R. H.; Khan, M. S.; Lewis, J. The Photovoltaic Effect in a Platinum Poly-yne. *Synth. Met.* **1994**, *67*, 245–249.

(52) Alvarado, S. F.; Seidler, P. F.; Lidzey, D. G.; Bradley, D. D. C. Direct Determination of the Exciton Binding Energy of Conjugated Polymers Using a Scanning Tunneling Microscope. *Phys. Rev. Lett.* **1998**, *81*, 1082–1085.

(53) Gregg, B. A.; Chen, S.-G.; Cormier, R. A. Coulomb Forces and Doping in Organic Semiconductors. *Chem. Mater.* **2004**, *16*, 4586–4599.

(54) Takeda, N.; Asaoka, S.; Miller, J. R. Nature and Energies of Electrons and Holes in a Conjugated Polymer, Polyfluorene. *J. Am. Chem. Soc.* **2006**, *128*, 16073–16082.

(55) Scholes, G. D. Insights into Excitons Confined to Nanoscale Systems: Electron–Hole Interaction, Binding Energy, and Photodissociation. *ACS Nano* **2008**, *2*, 523–537.

(56) Deibel, C.; Mack, D.; Gorenflot, J.; Schöll, A.; Krause, S.; Reinert, F.; Rauh, D.; Dyakonov, V. Energetics of Excited States in the Conjugated Polymer Poly(3-hexylthiophene). *Phys. Rev. B* **2010**, *81*, 085202.

(57) Kraabel, B.; Moses, D.; Heeger, A. J. Direct Observation of the Intersystem Crossing in Poly(3-octylthiophene). *J. Chem. Phys.* **1995**, *103*, 5102–5108.

(58) Monkman, A. P.; Burrows, H. D.; Hartwell, L. J.; Horsburgh, L. E.; Hamblett, I.; Navaratnam, S. Triplet Energies of  $\pi$ -Conjugated Polymers. *Phys. Rev. Lett.* **2001**, *86*, 1358–1361.

(59) Köhler, A.; Wilson, J. S.; Friend, R. H.; Al-Suti, M. K.; Khan, M. S.; Gerhard, A.; Bässler, H. The Singlet–Triplet Energy Gap in Organic and Pt-Containing Phenylene Ethynylene Polymers and Monomers. *J. Chem. Phys.* **2002**, *116*, 9457–9463.

(60) Scholes, G. D.; Rumbles, G. Excitons in Nanoscale Systems. *Nat. Mater.* **2006**, *5*, 683–696.

(61) Zhang, N.; Hayer, A.; Al-Suti, M. K.; Al-Belushi, R. A.; Khan, M. S.; Köhler, A. The Effect of Delocalization on the Exchange Energy in Meta- and Para-Linked Pt-Containing Carbazole Polymers and Monomers. *J. Chem. Phys.* **2006**, *124*, 244701.

(62) Milián-Medina, B.; Gierschner, J. Computational Design of Low Singlet–Triplet Gap All-Organic Molecules for OLED Application. *Org. Electron.* **2012**, *13*, 985–991.

(63) Wells, N. P.; Boudouris, B. W.; Hillmyer, H. A.; Blank, D. A. Intramolecular Exciton Relaxation and Migration Dynamics in Poly(3-hexylthiophene). *J. Phys. Chem. C* **2007**, *111*, 15404–15414.

(64) Xie, Y.; Li, Y.; Xiao, L.; Qiao, Q.; Dhakal, R.; Zhang, Z.; Gong, Q.; Galipeau, D.; Yan, X. Femtosecond Time-Resolved Fluorescence Study of P3HT/PCBM Blend Films. *J. Phys. Chem. C* **2010**, *114*, 14590–14600.

(65) Ferreira, B.; da Silva, P. F.; de Melo, J. S. S.; Pina, J.; Maçanita, A. Excited-State Dynamics and Self-Organization of Poly(3-hexylthiophene) (P3HT) in Solution and Thin Films. *J. Phys. Chem. B* **2012**, *116*, 2347–2355.

(66) Scholes, G. D.; Larsen, D. S.; Fleming, G. R.; Rumbles, G.; Burn, P. L. Origin of Line Broadening in the Electronic Absorption Spectra of Conjugated Polymers: Three-Pulse-Echo Studies of MEH-PPV in Toluene. *Phys. Rev. B* **2000**, *61*, 13670–13678.

(67) Tretiak, S.; Saxena, A.; Martin, R. L.; Bishop, A. R. Conformational Dynamics of Photoexcited Conjugated Molecules. *Phys. Rev. Lett.* **2002**, *89*, 097402.

(68) Yang, X.; Dykstra, T. E.; Scholes, G. D. Photon-Echo Studies of Collective Absorption and Dynamic Localization of Excitation in Conjugated Polymers and Oligomers. *Phys. Rev. B* **2005**, *71*, 045203.

(69) Ruseckas, A.; Wood, P.; Samuel, I. D. W.; Webster, G. R.; Mitchell, W. J.; Burn, P. L.; Sundström, V. Ultrafast Depolarization of the Fluorescence in a Conjugated Polymer. *Phys. Rev. B* **2005**, *72*, 115214.

(70) Dykstra, T. E.; Hennebicq, E.; Beljonne, D.; Gierschner, J.; Claudio, G.; Bittner, E. R.; Knoester, J.; Scholes, G. D. Conformational Disorder and Ultrafast Exciton Relaxation in PPV-family Conjugated Polymers. *J. Phys. Chem. B* **2009**, *113*, 656–667.

(71) Hwang, I.; Scholes, G. D. Electronic Energy Transfer and Quantum-Coherence in  $\pi$ -Conjugated Polymers. *Chem. Mater.* **2011**, *23*, 610–620.

(72) Ruseckas, A.; Theander, M.; Valkunas, L.; Andersson, M. R.; Inganäs, O.; Sundström, V. Energy Transfer in a Conjugated Polymer with Reduced Inter-Chain Coupling. *J. Lumin.* **1998**, *76–77*, 474–477.

(73) Grage, M. M.-L.; Pullerits, T.; Ruseckas, A.; Theander, M.; Inganäs, O.; Sundström, V. Conformational Disorder of a Substituted Polythiophene in Solution Revealed by Excitation Transfer. *Chem. Phys. Lett.* **2001**, *339*, 96–102.

(74) Westenhoff, S.; Daniel, C.; Friend, R. H.; Silva, C.; Sundström, V.; Yartsev, A. Exciton Migration in a Polythiophene: Probing the Spatial and Energy Domain by Line-Dipole Förster-Type Energy Transfer. *J. Chem. Phys.* **2005**, *122*, 094903.

(75) Westenhoff, S.; Beenken, W. J. D.; Friend, R. H.; Greenham, N. C.; Yartsev, A.; Sundström, V. Anomalous Energy Transfer Dynamics due to Torsional Relaxation in a Conjugated Polymer. *Phys. Rev. Lett.* **2006**, *97*, 166804.

(76) Westenhoff, S.; Beenken, W. J. D.; Yartsev, A.; Greenham, N. C. Conformational Disorder of Conjugated Polymers. *J. Chem. Phys.* **2006**, *125*, 154903.



(77) Scheblykin, I. G.; Yartsev, A.; Pullerits, T.; Gulbinas, V.; Sundström, V. Excited State and Charge Photogeneration Dynamics in Conjugated Polymers. *J. Phys. Chem. B* **2007**, *111*, 6303–6321.

(78) Yu, W.; Zhou, J.; Bragg, A. E. Exciton Conformational Dynamics of Poly(3-hexylthiophene) (P3HT) in Solution from Time-Resolved Resonant-Raman Spectroscopy. *J. Phys. Chem. Lett.* **2012**, *3*, 1321–1328.

(79) Magnani, L.; Rumbles, G.; Samuel, I. D. W.; Murray, K.; Moratti, S. C.; Holmes, A. B.; Friend, R. H. Photoluminescence Studies of Chain Interactions in Electroluminescent Polymers. *Synth. Met.* **1997**, *84*, 899–900.

(80) Beljonne, D.; Cornil, J.; Friend, R. H.; Janssen, R. A. J.; Brédas, J. L. Influence of Chain Length and Derivatization on the Lowest Singlet and Triplet States and Intersystem Crossing in Oligothiophenes. *J. Am. Chem. Soc.* **1996**, *118*, 6453–6461.

(81) Beljonne, D.; Shuai, Z.; Pourtois, G.; Brédas, J. L. Spin–Orbit Coupling and Intersystem Crossing in Conjugated Polymers: A Configuration Interaction Description. *J. Phys. Chem. A* **2001**, *105*, 3899–3907.

(82) Turro, N. J.; Ramamurthy, V.; Scaiano, J. C. *Modern Molecular Photochemistry of Organic Molecules*, University Science Books: Sausalito, CA, 2010.

(83) Rogers, J. E.; Cooper, T. M.; Fleitz, P. A.; Glass, D. J.; McLean, D. G. Photophysical Characterization of a Series of Platinum(II)-Containing Phenyl-Ethynyl Oligomers. *J. Phys. Chem. A* **2002**, *106*, 10108–10115.

(84) Guo, F.; Ogawa, K.; Kim, Y.-G.; Danilov, E. O.; Castellano, F. N.; Reynolds, J. R.; Schanze, K. S. A Fulleropyrrolidine End-Capped Platinum-Acetylide Triad: The Mechanism of Photoinduced Charge Transfer in Organometallic Photovoltaic Cells. *Phys. Chem. Chem. Phys.* **2007**, *9*, 2724–2734.

(85) Rogers, J. E.; Slagle, J. E.; Krein, D. M.; Burke, A. R.; Hall, B. C.; Fratini, A.; McLean, D. G.; Fleitz, P. A.; Cooper, T. M.; Drobizhev, M.; et al. Platinum Acetylide Two-Photon Chromophores. *Inorg. Chem.* **2007**, *46*, 6483–6494.

(86) Ramakrishna, G.; Goodson, T.; Rogers-Haley, J. E.; Cooper, T. M.; McLean, D. G.; Urbas, A. Ultrafast Intersystem Crossing: Excited State Dynamics of Platinum Acetylide Complexes. *J. Phys. Chem. C* **2009**, *113*, 1060–1066.

(87) Liao, C.; Yarnell, J. E.; Glusac, K. D.; Schanze, K. S. Photoinduced Charge Separation in Platinum Acetylide Oligomers. *J. Phys. Chem. B* **2010**, *114*, 14763–14771.

(88) Sheng, C.-X.; Singh, S.; Gambetta, A.; Drori, T.; Tong, M.; Tretiak, S.; Vardeny, Z. V. Ultrafast Intersystem-Crossing in Platinum Containing  $\pi$ -Conjugated Polymers with Tunable Spin-Orbit Coupling. *Sci. Rep.* **2013**, *3*, 2653.